

Improved ghost-correction in multi-shot EPI using PLACE and GESTE

W Scott Hoge^{1,2}, Huan Tan³, Robert A Kraft⁴, and Jonathan R Polimeni^{2,5}

¹Brigham and Women's Hospital, Boston, Massachusetts, United States, ²Harvard Medical School, Boston, MA, United States, ³Department of Surgery (Neurosurgery), University of Chicago, Chicago, Illinois, United States, ⁴Virginia-Tech Wake Forest School of Biomedical Engineering, Winston-Salem, NC, United States, ⁵A.A. Martinos Center for Biomedical Imaging, MGH, Charlestown, MA, United States

Target Audience: Physicists/Engineers that develop multi-shot EPI applications.

Purpose: EPI is widely used in functional neuroimaging studies because it provides rapid data acquisition for various functional contrasts. While a stack of 2D EPI images can image the whole brain within 1–2 s, EPI is vulnerable to inherent artifacts that degrade image quality. In particular, static local field inhomogeneity and eddy current effects induced by the EPI readout often produce Nyquist ghosting, geometric distortion, and signal loss in regions of magnetic susceptibility gradients.

One mechanism to reduce these effects is to use multi-shot EPI—splitting the data acquisition over multiple excitations/readouts. This reduces the vulnerability of EPI to static field effects that cause artifacts and distortion, while ghosting can increase as phase errors must be corrected both within and across each segment. In order to reduce residual ghosting in multi-shot EPI data, we propose the use of temporal encoding and a PLACE-like¹ or GESTE-like² strategy to perform robust phase correction between segments during image reconstruction. Both PLACE and GESTE have been previously shown to provide superior EPI Nyquist ghost suppression caused by readout gradient mismatch in single-shot EPI data. These methods are extended here to phase-correct multi-shot EPI data.

Methods: We implemented temporal encoding in a multi-shot gradient-echo segmented EPI sequence, enabling pairs of segments to be acquired with opposite polarity readout gradients. Each segment is first acquired using a positive readout gradient for the first sampled line in the EPI echo train, and then the same segment is acquired again using a negative readout gradient for the first line.

The basic blocks to combine multi-shot EPI data are: ghost-correct the EPI data within each segment; phase correct across segments; combine to form the final image. We examined three approaches that perform each of the aforementioned functions in slightly different ways using temporally encoded data.

The first strategy evaluated here follows a PLACE-like approach. Data from each segment are split into one set acquired on positive readout (RO+) gradients, and one acquired on negative readout (RO-) gradients. All RO+ data from all segments are then combined to form an un-aliased image data set, and all RO- data from all segments are combined to form a second un-aliased set. The first-order (1D linear) and scalar phase differences along the readout direction between these two images are corrected as in GESTE², and the images are added together. Images from this method are labeled “A” in the figures.

For the second strategy, first *each segment pair* is interleaved and combined to form one set of data with RO+ samples, and a second set of data with RO- samples. The data are then Fourier transformed to the image domain via a 2D FFT. The sets are then phase matched as above, and coherently combined to form a ‘ghost-free’—but aliased—image. After correcting for a scalar phase differences between the segments, the segments are combined into an un-aliased image. This method is shown as image “B” in the figures.

The third and final strategy we evaluated applies a GESTE-style approach, which is applicable with data from multi-channel coils. Here, we use the data from the method A to generate GRAPPA reconstruction coefficients which are then applied to each segment in B to generate un-aliased images at the full resolution. Images from one segment at this stage are shown as image “C” in the figures. Finally, these un-aliased images from each segment are phase matched and coherently combined to form the final image. We note that the parallel imaging artifact cancellation reported by the authors of [2] in single-shot EPI holds true in multi-shot images as well. This method is shown as image “D” in each of the figures.

Results: Temporally encoded *in-vivo* data were collected from a healthy normal volunteer on a Siemens 7T whole-body scanner equipped with an SC72 gradient coil and a 32-channel helmet RF array coil with parameters: 4 segments; TR: 2 s; TE: 26 ms; echo spacing: 0.79 ms; flip angle: 75°; matrix size: 174 × 174; slices: 34; resolution: 1.1 mm isotropic. Images from two coils are shown in Fig. 1, where the windowing has been adjusted to emphasize ghosting. It is notable here that residual ghosts can be seen (as indicated by the arrows) in methods A and B that rely on PLACE alone. Method C relies on these images as well, and thus some errors are carried forward when PLACE-corrected images are used to calibrate the GRAPPA coefficients that are applied to each segment. The GESTE-based method D, which benefits from greater coherent averaging, shows a significant absence of ghosting in these same coils.

Fig. 2 illustrates the final image using root-sum-of-squares for coil combination. Images with standard windowing are shown on the left. These images are windowed to the lowest 10% of signal range on the right, which again shows visible ghosting in Methods A and B. The lack of ghosting is again most apparent in the image from the GESTE-based method D.

Discussion: We have demonstrated that a GESTE-based approach to reconstruct data from multi-shot EPI can dramatically reduce the level of residual ghosting in the final image. We anticipate this method to show the greatest benefit in images used for the calibration of parallel imaging methods such as SENSE and GRAPPA, as accelerated EPI is particularly sensitive to ghosting errors in the parallel imaging calibration data.

References: [1] Xiang and Ye. *MRM* 2007; 57(4):731–41. [2] Hoge, Tan, and Kraft. *MRM* 2010; 64(6):1781–91. **Supported by:** NIBIB K01-EB011498.

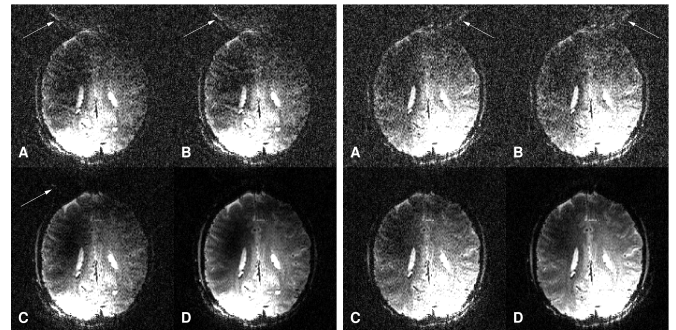


Fig 1: Images from two coils for Methods A-D

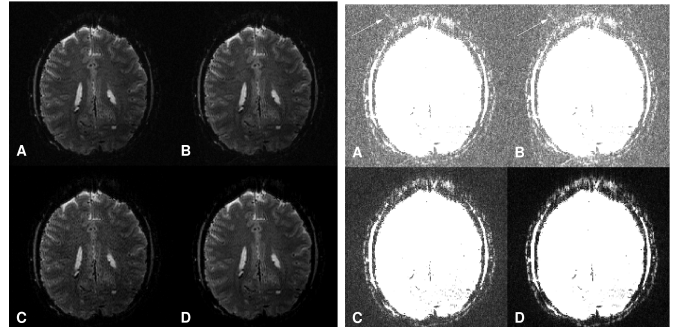


Fig 2: RSOS Images for Methods A-D. left: normal windowing, right: windowed to emphasize ghosting.